IEEE Photonics Journal
An IEEE Photonics Society Publication

Open Access

High-Quality Optical Frequency Comb by Spectral Slicing of Spectra Broadened by SPM

Volume 5, Number 5, October 2013

D. Hillerkuss
T. Schellinger
M. Jordan
C. Weimann
F. Parmigiani
B. Resan
K. Weingarten
S. Ben-Ezra
B. Nebendahl
C. Koos
W. Freude
J. Leuthold

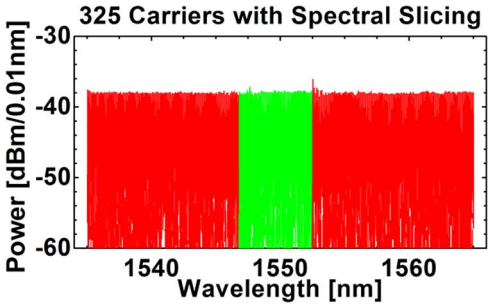

DOI: 10.1109/JPHOT.2013.2280524
1943-0655 © 2013 IEEE

IEEE photonics SOCIETY

IEEE

High-Quality Optical Frequency Comb by Spectral Slicing of Spectra Broadened by SPM

D. Hillerkuss,[1] T. Schellinger,[2] M. Jordan,[2] C. Weimann,[2] F. Parmigiani,[3] B. Resan,[4] K. Weingarten,[4] S. Ben-Ezra,[5] B. Nebendahl,[6] C. Koos,[2] W. Freude,[2] and J. Leuthold[1,2]

[1]Institute of Electromagnetic Fields (IFH), ETH Zurich, 8092 Zurich, Switzerland
[2]IPQ and IMT, Karlsruhe Institute of Technology (KIT), 76131 Karlsruhe, Germany
[3]Optoelectronics Research Centre, University of Southampton, Southampton, SO17 1BJ, U.K.
[4]Time-Bandwidth Products, 8952 Zurich, Switzerland
[5]Finisar Corporation, Nes Ziona 74140, Israel
[6]Agilent Technologies, 71034 Boeblingen, Germany

DOI: 10.1109/JPHOT.2013.2280524

Manuscript received July 30, 2013; accepted August 21, 2013. Date of publication September 4, 2013; date of current version September 17, 2013. This work was supported in part by the European FP7 projects ACCORDANCE (FP7-ICT-2009-4) and FOX-C (FPC-ICT-2011-8), by the Agilent University Relations Program, by the German BMBF project CONDOR (BMBF 16BP1015), by the Helmholtz International Research School of Teratronics, by the Karlsruhe School of Optics and Photonics (KSOP), and by the German Research Foundation (DFG). Corresponding author: D. Hillerkuss (e-mail: dhillerkuss@ethz.ch).

Abstract: This paper introduces a spectral slicing technique that extends the useful spectral range of frequency combs generated through self-phase modulation (SPM) of mode-locked laser pulses. When generating frequency combs by SPM, the spectral range with high-quality carriers is usually limited due to spectral minima carrying too little power. To overcome these limitations, we combine suitable slices of broadened and nonbroadened spectra. The concept was experimentally verified: A total number of 325 consecutive equidistant subcarriers span a bandwidth of 4 THz. All subcarriers have an optical carrier-power-to-noise-power-density ratio (OCNR) larger than 25.8 dB (0.1 nm) and were derived from one mode-locked laser with a mode linewidth of approximately 1 kHz. The signal quality of the comb and in particular of each subcarrier was ultimately tested in a terabit-per-second communication experiment. The comb quality allowed us to transmit 32.5 Tb/s over 225 km with 100 Gb/s dual polarization 16-ary quadrature amplitude modulation (16QAM) signals on each of the subcarriers.

Index Terms: Fiber nonlinear optics, optical fiber communication, optical pulses, supercontinuum generation.

1. Introduction

Optical frequency combs that offer hundreds of carriers of highest quality across a large spectral band have drawn a tremendous amount of attention within recent years. Research on frequency combs culminated in the Nobel Price that was awarded to John Hall and Theodor Hänsch in 2005 for their work in laser-based precision spectroscopy [1], [2]. Optical frequency combs were recognized as a useful tool not only for spectroscopy but also for various other applications such as optical and microwave waveform generation [3], [4], optical signal processing [5], [6], fiber-optic communication [7]–[17], optical coherence tomography [18], and precision ranging [19]. Depending on the application, the individual linewidth, the line spacing or the total number of lines (e.g., spanning an octave for self-referencing) are important and ultimately influence the design.

Optical frequency combs are most attractive for the latest generation of optical multi-carrier communication systems, where information is encoded in so called superchannels. To generate Tbit/s superchannels, data is encoded on multiple closely spaced, equidistant optical carriers and subsequently multiplexed. Such systems require a precisely controlled carrier spacing, which is inherently provided by optical comb sources. Here, a single comb source could replace hundreds of lasers, which would otherwise have to be controlled precisely in their relative and absolute frequencies. Prominent examples of such superchannel communication systems are based on all-optical orthogonal frequency division multiplexing (OFDM) [16], no guard interval OFDM [20], coherent wavelength division multiplexing (Co-WDM) [9], and Nyquist WDM [8], [21]–[23]. However, such schemes require a precise control of carrier frequencies [9], [16], [20]–[22], and in rare cases even of the carrier phases with respect to the symbol time slot [9]. Fortunately, in optical frequency comb sources, the carrier spacing is extremely precise, and strictly linear time dependencies of the phases between carriers are maintained, making them ideally suited for this application.

However, in order to use the carriers of an optical frequency comb for communications they must have a sufficiently narrow spacing (e.g., 12.5 or 25 GHz) and offer sufficient quality. This actually means that

- All the optical carriers should be of equal power (or follow a defined spectral distribution). This is needed to achieve a similar performance of the data encoded on the carriers and to avoid one modulated carrier limiting the performance of all neighbors through crosstalk. Equal power in all carriers typically can be achieved through equalization of a generated frequency comb [14], [16].
- The carriers must have a minimum carrier-power to noise-power-density ratio (CNR). The CNR ultimately limits the amount of information that can be encoded on a single subcarrier. The CNR directly defines the maximum achievable signal-to-noise ratio (SNR), for which minimum values can be found in tables.
- The linewidth of all carriers has to be narrow. A narrow linewidth (low phase noise) is fundamentally needed—particularly for transmission systems making use of phase encoded signals. Coherent transmission systems typically need a laser linewidth that is significantly smaller than 100 kHz.

Quite a few schemes have been experimentally investigated for use in optical communication systems that can fulfill these requirements to a smaller or larger extent. Among these are comb generators based on optical modulators [9], [10], [24], also in the form of recirculating frequency shifters [7], [11], [12], micro resonators [15], [25], [26], and mode-locked lasers (MLL) with spectral broadening in highly nonlinear fibers (HNLF) [13], [14]. All these schemes have different advantages and drawbacks: Schemes using modulators typically have a sufficient carrier quality but only offer a few lines and the operation points of the modulators have to be controlled precisely. Schemes that exploit self-phase modulation (SPM) typically provide a sufficient number of subcarriers, but the CNR is low at the spectral minima and at the outer edges of the spectrum.

In this paper, we present a comb generator scheme based on slicing of spectra broadened in highly nonlinear fibers. The scheme extends the usable bandwidth of frequency combs generated through SPM by removing the minima [27] in broadened spectra. The scheme promises a large number of carriers with ample power and CNR for optical transmission systems by spectrally composing suitable subspectra [16]. In our demonstration, we generate a total number of 325 carriers, which we derived from a single MLL. The MLL was measured to provide a linewidth of approximately 1 kHz. The CNR of all carriers of the frequency comb was larger than 25.8 dB and the quality was proven in a transmission experiment.

2. Spectral Minima in Self-Phase Modulation

Spectral broadening through self-phase modulation (SPM) can generate extremely broad frequency combs. However, as already observed by Stolen *et al.* in 1978 [27], spectral minima occur for phase shifts significantly larger than π. Typically, these minima are explained as destructive interference of spectral components that have experienced a relative phase shift of π [28].

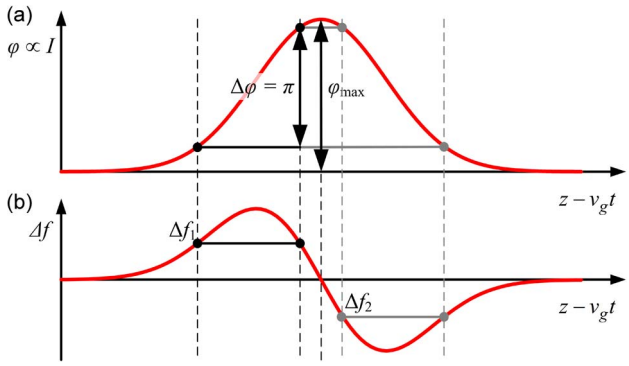

Fig. 1. Schematic phase and frequency shift in self-phase modulation of a single impulse with intensity I in a moving time frame z–$v_g t$ (propagation coordinate z, time t, group velocity v_g). (a) Nonlinear phase shift $\varphi \propto I$. The phase shift has a maximum φ_{max} at the peak of the pulse and translates to a frequency shift Δf as seen in (b). In a simplified picture, each frequency shift occurs twice within one pulse (see example in this figure), but with a different phase. If the maximum phase shift φ_{max} is larger than π, there will be at least two pairs of points (Δf_1 and Δf_2), one with a positive Δf_1 and one with a negative frequency shift Δf_2, which have a phase difference of $\Delta\varphi = \pi$. This phase shift then leads to spectral destructive interference at these frequency shifts Δf_1 and Δf_2. In our example these frequency shifts are symmetric around $\Delta f = 0$, which is not necessarily the case for asymmetric impulses or in the presence of dispersion.

In a simplified picture, the generation of the spectral minima in SPM can be illustrated as shown in Fig. 1. The intensity of an optical impulse is displayed in a moving time frame z–$v_g t$ (group velocity v_g) along the propagation direction z, Fig. 1(a). Due to the Kerr nonlinearity, the optical phase shift $\varphi \propto I$ is in proportion to the local intensity I. The slopes of the impulse lead to a frequency offset Δf, Fig. 1(b). If the maximum phase shift φ_{max} is larger than π, then above (and also below) $\Delta f = 0$ there will be pairs of points with the same Δf but a relative phase shift $\Delta\varphi = \pi$. In this simple picture, this will lead to destructive interference of these spectral components, and therefore to minima in the spectrum. In our example, these frequencies are labeled Δf_1 and Δf_2.

Fig. 2 presents simulated and measured power spectra that exhibit these minima. The simulated example spectra Fig. 2(a) are computed for a single spectrally broadened pulse. If $\Delta\varphi \geq \pi$, spectral minima develop. As seen in the figure, the number of minima m allows for an estimation of the maximum phase shift φ_{max} according to

$$\varphi_{max} \approx \frac{2m+1}{2}\pi. \tag{1}$$

This equation is related to the equation (4.1.14) in [28], which gives a similar relation for the number of spectral maxima resulting from a certain maximum phase shift.

The measurement in Fig. 2(b) relates to the mode locked laser (MLL) with a repetition rate $R = 12.5$ GHz, which was used for all experiments in this paper. Its comb line spectrum was amplified to the specified average powers and broadened by SPM. The minima are marked with white symbols "v". Because interference is involved, any instability in the optical MLL power leads to a frequency shift of these minima, and therefore to a pronounced instability of the neighboring comb lines.

3. Comb Generation by Spectral Slicing

The following scheme generates a frequency comb with a large bandwidth and a high carrier quality for all carriers. We propose to compose this high quality frequency comb from a seed spectrum and one or more broadened spectra [16]. We replace carriers at spectral minima of broadened spectra with a low carrier power and CNR by carriers from differently broadened spectra with a high carrier quality. This process has the four steps shown in Fig. 3. First, we generate the seed spectrum using an optical pulse source, such as a MLL. From this seed spectrum, we then generate N optical

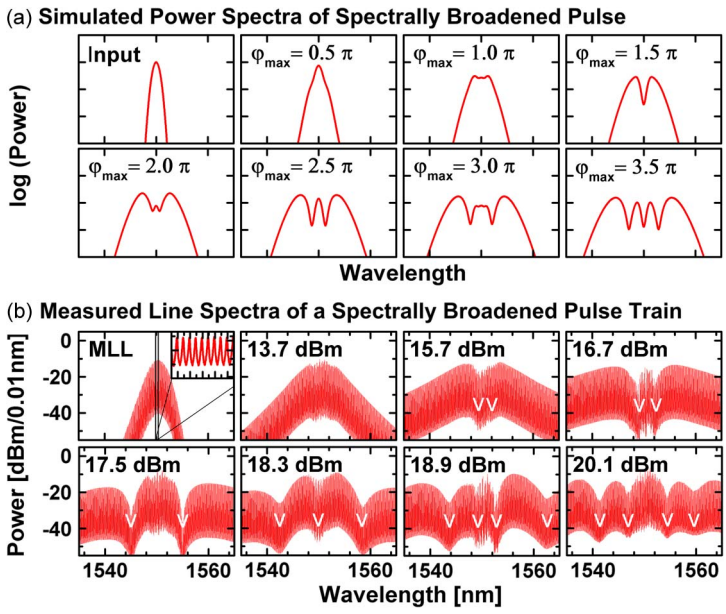

Fig. 2. Simulated and measured spectra for spectral broadening through self-phase modulation in a highly nonlinear fiber. (a) Single pulse with its spectrum labeled "input". After spectral broadening in a highly nonlinear fiber (HNLF), the maximum nonlinear phase shift is φ_{max}. It increases proportional to the input power, which increases from left to right and from upper to lower row. The spectra exhibit minima for maximum nonlinear phase shifts significantly larger than π [27]. (b) Non-broadened line spectrum of the mode locked laser (MLL), and line spectra broadened by SPM in the HNLF. The average input power to the HNLF is given in dBm. Spectral minima are marked with a white "v". For higher powers, not all minima are within the displayed bandwidth of 30 nm. The spectra were measured at the output of the HNLF in the setup seen in Fig. 4.

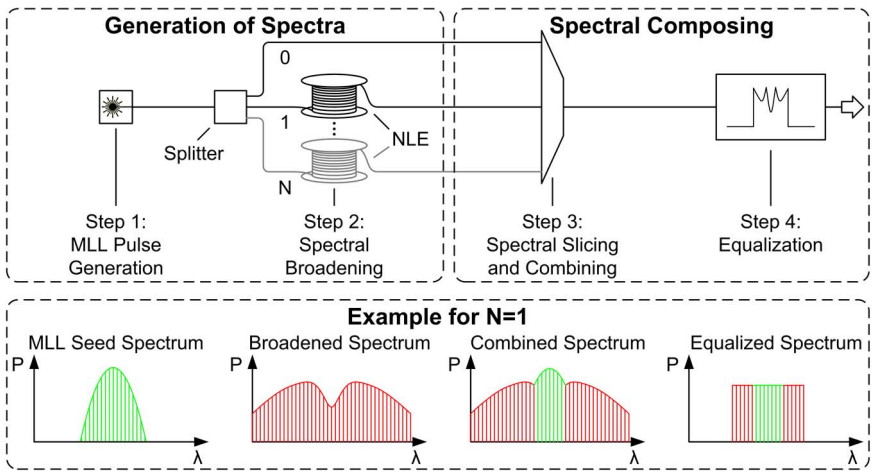

Fig. 3. Concept of the optical comb generator by spectral slicing. First, *N* optical spectra are generated; a mode locked laser (MLL) generates the initial seed spectrum (as shown in green) that is spectrally broadened in a nonlinear element (NLE) to generate *N* broadened spectra with a large number of carriers (as shown in red). Second, the output spectrum is generated from the *N* spectra using spectral slicing and composing; for this, the generated spectra are sliced and combined to form a wide spectrum. This wide spectrum is subsequently equalized to obtain the output spectrum of the comb generator. The lower part in this figure shows exemplary spectra for two combined optical spectra.

spectra via spectral broadening elements (NLE), such as a highly nonlinear fiber (HNLF). Next, we use spectral slicing and composing in a reconfigurable optical multiplexer (e.g., waveshaper). Here, the usable parts of the seed spectrum and the *N* additional spectra are sliced and combined to form

a continuous broad output spectrum. This effectively replaces all unstable and low-power parts of the optical spectra. Finally, the spectrum is equalized. The bottom inset in Fig. 3 illustrates this process for $N = 1$.

For current implementations of this scheme with discrete components, the following points have to be kept in mind as they could limit the overall performance and/or usability for different applications:

- A poor filter-stop band could limit the performance in several ways.
  - As a result of a poor filter-stop band multipath interference between carriers from different paths $0, 1, \ldots N$ in Fig. 3 could lead to low frequency fluctuations in the kHz range due to thermal path length changes. This could result in phase and amplitude fluctuations of the comb lines. This did not pose an issue in our experiments as the 40 dB filter extinction ratio of the waveshaper was sufficient as outlined in Section 4.
  - The filter's extinction ratio often is not sufficient at the edge of the filters when going from stop-band to pass band. In our experiment we indeed noticed some small crosstalk in the two lines where spectral slices are merged. However, this multipath interference should not be mistaken for coherent crosstalk in communication systems [29], as the interfering laser lines do not carry any data at that point. And indeed, in our case it did not lead to any signal degradation.
  - A poor filter-stop band could also degrade the overall CNR as a result of summing up noise floors from different paths. This however is quite unlikely, as the noise floor of the interfering spectrum would have to be much higher than the noise floor in the desired spectrum as it is attenuated by the filter extinction. In our experiment this was most definitely not an issue as we started with a very good CNR that was further suppressed in the filters.
- As the different paths in the comb generator consist of different lengths of fiber, a decorrelation of the different segments of the comb could occur if the lengths are equal to or larger than the coherence length. This could lead to very small frequency shifts between spectral comb slices if the center frequency of the source laser drifts. Due to the short fiber length of 100 m and a coherence length in the order of 100 km, this was no issue in our experiments.

Of course, in an ultimate integrated solution, the best stability could be by achieved by miniaturization that includes on chip nonlinear elements instead of HNLFs.

4. Experimental Setup of the Broadband Spectrally Sliced Comb Source

Fig. 4 shows our experimental setup. A passively mode locked laser (MLL—Ergo XG) with a repetition rate of 12.5 GHz and a pulse width below 2 ps generates the initial seed spectrum [Fig. 4(a)]. The spacing of the spectral lines equals the repetition rate, while the pulse width and shape determine the spectral envelope. The chirp of the MLL is adjusted by 5.4 m of standard dispersion compensating fiber (DCF). Different fiber lengths were tested, and the length generating the largest amount of SPM at the output of the HNLF was chosen for the experiment. The spectrum is amplified, and a 5 nm bandpass filter suppresses the amplifier noise. The laser signal is now split in two parts. One part is spectrally broadened by SPM [see Fig. 4(b)] in a highly nonlinear photonic crystal fiber (HNLF). The HNLF is a photonic crystal fiber with the following parameters: length 100 m, dispersion 1.25 ps/nm/km, mode field diameter 2.8 $\pm$ 0.5 μm, attenuation $<$ 9 dB/km, nonlinear coefficient 19 W^{-1} km^{-1}. The other part is not broadened; instead, it is just passed through. Finally, the waveshaper slices, combines, and equalizes the broadened and the original MLL spectrum, thus producing the final output spectrum, Fig. 4(c). To show the suppression and estimate possible fluctuations of the power in individual lines, we have performed the measurement shown in Fig. 4(d). The most critical carriers are the carriers at the edges, where we only achieve a suppression of $>$ 16 dB. All other carriers have a suppression $>$ 30 dB and typically 40 dB. This corresponds to a power fluctuation of $<$ 3 dB for the carriers at the edges and a fluctuation of $<$ 0.6 and typically $<$ 0.2 dB for the central carriers. The speed of these fluctuations only depends on linewidth and frequency stability of the MLL and the stability of the interferometer. In our experiment, these fluctuations were extremely slow due to the high stability of the MLL.

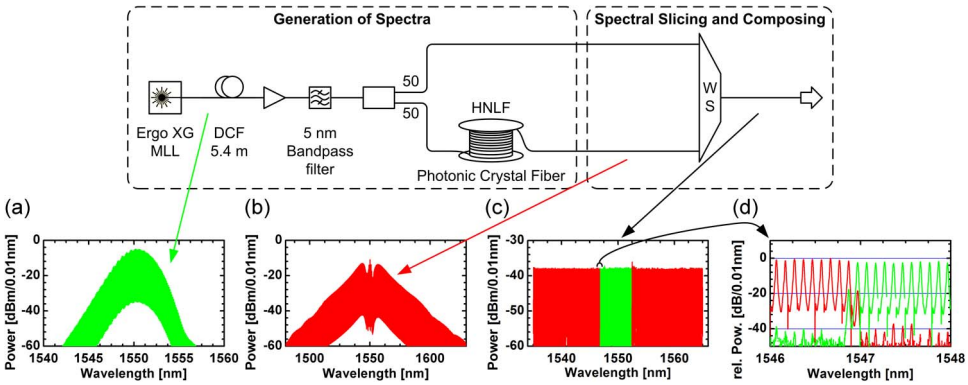

Fig. 4. Experimental setup of the ultra-broad spectrally sliced comb. The output spectrum of the mode locked laser (MLL—Ergo-XG, repetition rate 12.5 GHz) is displayed in the first inset (a—shown in green). The MLL pulses are amplified and filtered in a 5 nm bandpass filter. The amplified pulses are split, and one path is passed through and the other path is spectrally broadened in a highly nonlinear photonic crystal fiber (b—shown in red—HNLF). A waveshaper (WS) performs the spectral slicing and composing to generate the output spectrum (c—shown in green and red). The suppression of the neighboring spectra at one of the edges is shown (d). The suppression at the carriers next to the edges is > 16 dB. For all other carriers, a suppression > 30 dB, typically 40 dB is achieved.

The resulting flat frequency comb shown in Fig. 4(c) has 325 high-quality carriers that have been used for multiple Terabit/s transmission experiments [8], [16] with aggregate data rates of up to 32.5 Tbit/s [8]. In these experiments, we carefully measured data transmission on each and every spectral line of the generated frequency comb. We observed a similar performance for all subcarriers and did not see any impact of multipath interference [8], [16].

5. Characterization

5.1. Linewidth Characterization of the Mode Locked Laser

The linewidth of the individual modes of the MLL fundamentally limits the linewidth of the carriers in the broadened comb. We therefore measured the linewidths of five modes of the MLL, which we found to be approximately 1 kHz. We were limited to these five modes around 1550 nm due to the fixed wavelength of the narrow linewidth reference laser.

The linewidth of lasers is often measured using a delayed self-heterodyne technique [30], [31], in which the laser is split and one copy is decorrelated in a fiber delay line before being mixed with the original laser line. However, from our transmission experiments with this comb source [8], we expect an extremely low linewidth. This would results in an excessively long fiber length required for decorrelation [30]. Such a long fiber delay renders self-heterodyne measurements extremely susceptible to acoustic noise and other environmental influences. As such types of noise have significant frequency components in the same order of magnitude as the linewidth of interest, self-heterodyne measurements were not practical.

We therefore chose to measure the linewidth through a heterodyne measurement [31]. Normally, one would perform the measurement by combining the laser line under test with a narrow linewidth laser (NLWL) and then detecting the signal in a photodiode. The photocurrent is then analyzed in an RF-spectrum analyzer. However, due to the low measurement speed of these analyzers, this scheme requires wavelength tracking to compensate for slow drifts of the laser wavelengths [31]. Therefore, we decided for a new technique. To measure the linewidth of the laser without the drift of the laser wavelengths we chose to perform the measurement using real-time acquisition and subsequent spectral analysis of the recorded signal, see Fig. 5(c). In this scheme we used a coherent receiver (Agilent optical modulation analyzer) with a narrow linewidth laser (NLWL) as external local oscillator (LO). The receiver has an electrical bandwidth of 32 GHz per in-phase and

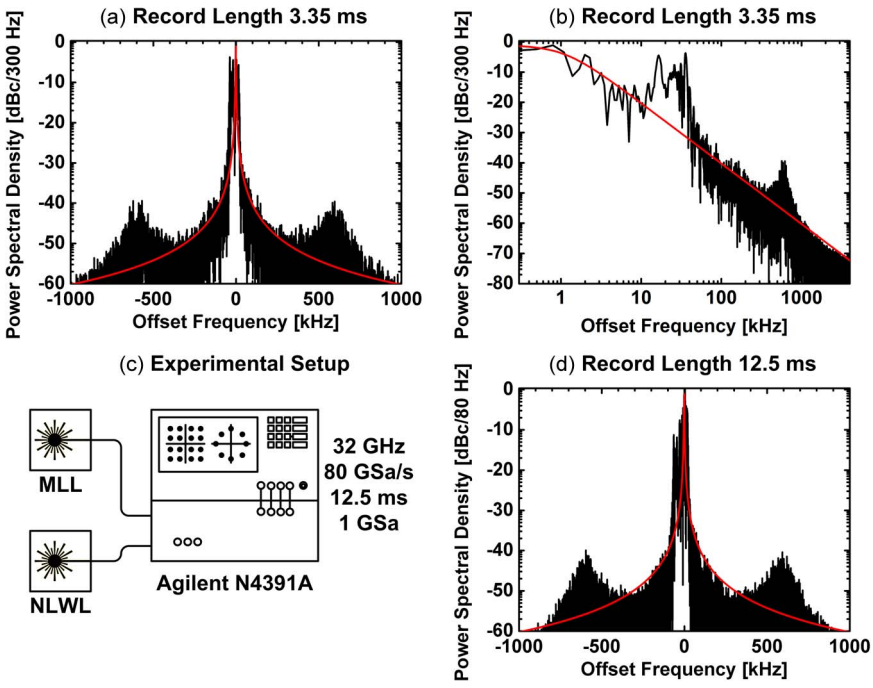

Fig. 5. Linewidth characterization of the mode locked laser (MLL). As shown in the bottom left subfigure (c), the mode locked laser (MLL) is recorded for 12.5 ms in a coherent receiver. The local oscillator is a narrow linewidth laser (NLWL) with a linewidth of approximately 1 kHz. The upper two subfigures (a), (b) display the power spectral density (shown in black) of one of the MLL lines mixed with the NLWL in an observation interval of 3.35 ms. The full width half maximum (FWHM) of the measured spectrum is less than 2 kHz, while the FWHM of the Lorentzian fit (shown in red) is 2.2 kHz. Side peaks at $\pm$590 kHz are visible in addition to the Lorentzian line shape. The frequency drift dominates the spectrum for a longer record length of 12.5 ms (d). As reference, we also display the Lorentzian fit obtained from the shorter record length.

per quadrature channel and a sampling rate of 80 GSa/s per channel. The NLWL had a linewidth of approximately 1 kHz, and the down-converted optical pulse train of the MLL was recorded for a time span of 12.5 ms. The advantage of this new technique is that we can restrict the data acquisition to a time interval within which the relative laser frequency drift is significantly smaller than the linewidth. This way there is no need for performing active wavelength tracking even though the frequency might drift over several kHz within a few seconds. This slow frequency drift, however, is not critical for optical communication systems, as the frequency offset compensation in coherent receivers can easily compensate for it.

First, we analyze a subset of 2^{28} samples (3.35 ms). Within this short time window, the influence of frequency drift of the two lasers is marginal. After performing a fast Fourier transform (FFT) on the temporal data, we analyze each of the 5 MLL lines within the receiver bandwidth of 64 GHz centered on 1550 nm. To this end, we process spectra with a width of 2^{15} samples ($\sim$9.8 MHz) centered at each MLL line. All spectral lines look alike, so that we only picture one line in Fig. 5. The full-width half-maximum (FWHM) of the power spectra of all five analyzed lines is found to be 1.9 kHz. The FWHM of a Lorentzian fit, red lines in Fig. 5(a), (b), and (d), is 2.2 kHz. Because the sidelobes at $\pm$590 kHz were included in the fitting process and because of the limitation in the sampling duration and the 1 kHz linewidth of the reference laser, the inferred line width is a worst-case estimate of the actual 3 dB bandwidth.

Next, we process the full data set. In this case, the spectra are distorted by the drift of the two lasers, Fig. 5(d). For the recorded 5 MLL lines we observe linewidths between 260 Hz and 1.33 kHz. From these measurements, we conclude that the characterized modes of the MLL have a linewidth of approximately 1 kHz. The sidelobes to be seen in Fig. 5 were also observed when investigating

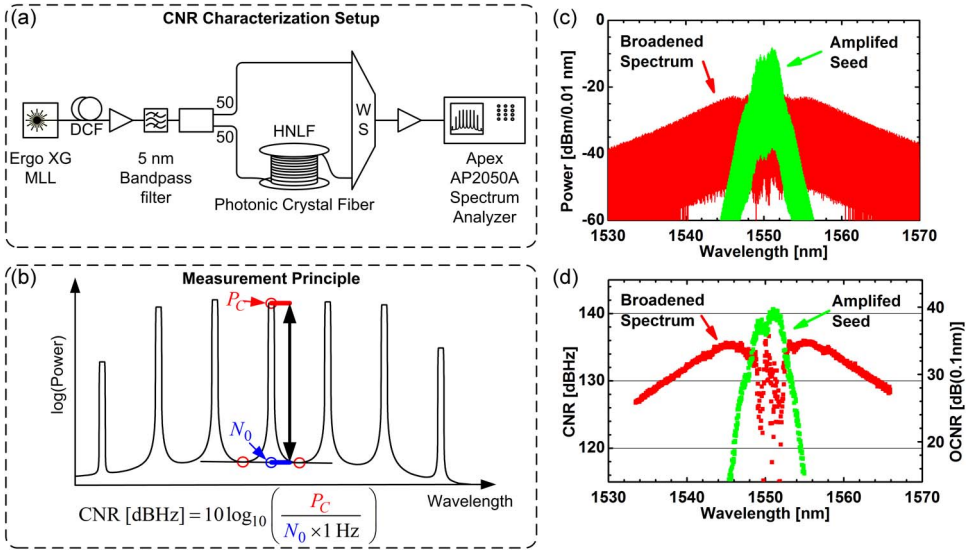

Fig. 6. Carrier-power to noise-power-density ratio (CNR) characterization of the comb source. (a) For the characterization of the CNR, the generation of spectra is implemented as illustrated in Fig. 4. Instead of equalization and spectral slicing, the waveshaper (WS) extracts 60 GHz out of the generated spectra (see top right) around the carrier to be characterized. A low noise EDFA amplifies the excerpt for characterization in the Apex AP2050A high resolution spectrum analyzer. The CNR is measured as illustrated in (b). The peak of the carrier is measured and the noise is determined by pseudo linear interpolation between the minima between the measured carrier and its neighbors. The obtained CNR values are shown in the plot (bottom right).

the MLL spectra with self-heterodyne measurements. However, due to environmental fluctuations, this measurement was not suitable for determining the linewidth.

5.2. CNR and OCNR Characterization of the Comb Source

The signal-to-noise ratio (SNR) and therefore the minimum carrier-power to noise-power-density ratio (CNR) have to be as large as possible in order to allow for reliable transmission of information.

We first implemented the comb source to study advanced multiplexing schemes at aggregate data rates beyond 10 Tbit/s [8], [16]. When investigating the noise characteristics in these experiments, we observed circular noise "clouds" around all constellation points. A statistical analysis of the error vector pointing from a nominal constellation point to the momentarily received signal yields the distribution of the noise in the system. From our statistical analysis in [8], we inferred a Gaussian distribution of the corresponding noise [8]. We conclude from these observations that the limiting factor for the signal quality is additive Gaussian noise due to amplified spontaneous emission in the optical amplifiers in the system, and not the phase noise of the optical carriers themselves. In the presence of significant phase noise the distribution of the received constellation points would have been distorted in an angular direction.

Next, we measured the CNR of the optical comb source. The CNR is defined as the ratio of the carrier-power P_C and the noise-power-density N_0 at the position of the carrier

$$\mathrm{CNR\ \ [dBHz]} = 10\log_{10}\left(\frac{P_C}{N_0 \Delta f}\right). \tag{2}$$

Here, the noise power density N_0 is normalized to a bandwidth of $\Delta f = 1$ Hz.

Characterization setup, measurement principle, and results of the CNR measurement are shown in Fig. 6. To measure the noise floor between the carriers with a spacing of 12.5 GHz, we used a high resolution optical spectrum analyzer (Apex AP2050A). The comb generated by spectral slicing

has been implemented as described in Section 4 and Fig. 4. The waveshaper (WS) now serves a different purpose. It is programmed to realize a bandpass filter function with a 3 dB bandwidth of 60 GHz. The center of the bandpass coincides with the carrier of interest. The filtered spectrum is then amplified in a low noise EDFA (not depicted in Fig. 4, noise figure NF $=$ 3.7 dB) to increase the power of the measured noise to a value significantly larger than the receiver noise of the spectrum analyzer. To ensure that the measurement is not limited by the electronic noise of the spectrum analyzer, the spectra are measured with three different resolution bandwidths of 50 pm, 20 pm, and 10 pm. The noise level at the carrier frequency is determined by linear interpolation between the noise levels on both sides of the carrier, see illustration in Fig. 6(b). All noise density measurements are normalized to a reference bandwidth of 1 Hz. Noise density measurements with different resolution bandwidths deviated by less than 0.6 dB, therefore electronic noise had only minimal influence on the measurement. Both, the amplified seed and the broadened spectrum, were present at the waveshaper inputs simultaneously during the CNR measurements.

In optical communication systems, a commonly used measure for communication signals is the optical signal-to-noise ratio (OSNR), which is given as the signal power in relation to the noise power density normalized to a bandwidth of 0.1 nm. This measure was established for historic reasons as 0.1 nm used to be the minimum resolution of optical spectrum analyzers. We therefore also provide the OCNR

$$\text{OCNR} \quad [\text{dB}(0.1nm)] = 10\log_{10}\left(\frac{P_C}{N_0}\frac{\lambda_c^2}{c\ \Delta\lambda_{\text{ref}}}\right) \tag{3}$$

with the speed of light c. Here, the noise-power density is normalized to a bandwidth of $\Delta\lambda_{\text{ref}} = 0.1$ nm at a reference wavelength $\lambda_c = 1550$ nm.

The CNR (and OCNR values) of the amplified seed spectrum, see green range in Fig. 6(d), is larger than 133.5 dBHz—reference bandwidth 1 Hz (32.5 dB (0.1 nm)—reference bandwidth 0.1 nm) in the center region of the flattened comb—the green part in Fig. 4(d). It varies between 114 dBHz (13 dB (0.1 nm)) and 140.6 dBHz (39.6 dB (0.1 nm)) over the measured bandwidth of 9.5 nm—here, we measured the CNR also measured across the spectral lines that were removed by the filter. The CNR of the broadened spectrum—the red part that was used to generate the spectrum in Fig. 4(d) and without the central green part—varies between 126.8 dBHz (25.8 dB (0.1 nm)) and 136 dBHz (35 dB (0.1 nm)). The CNR of the broadened spectrum that was replaced by the amplified seed spectrum was measured as well. We found that the CNR in this region was heavily fluctuating as one would expect from our discussion in Section 2. As a result we found scattered red dots as seen in Fig. 6(d). It should be mentioned that we sliced the spectrum at the points, where the carriers of the amplified seed and the broadened spectrum had a similar CNR and also a similar power. The plots in Fig. 6(c) and (d) also show that there was a strong correlation between the CNR and the power of the individual lines.

One might argue that this measurement scheme might underestimate the CNR for real operating condition, as the central part of the comb is attenuated by up to 25 dB and noise crosstalk from the inner part of the broadened spectrum might occur. This is not the case. The input spectrum to the HNLF has the same power as the input to the waveshaper for the center part of the spectrum. Therefore, the noise levels in between the lines for both spectra are similar. This crosstalk noise is at least 20 dB below the noise of the attenuated original spectrum due to the additional insertion loss of the HNLF ($>$ 5 dB) and the extinction of the waveshaper ($>$ 40 dB).

To put these numbers in relation, we provide the required SNR for transmission of two of the most common modulation formats for current and next generation communication systems. The SNR needed to transmit a polarization multiplexed 12.5 GBd QPSK or 16QAM signal with a bit error ratio of 2×10^{-3} is 10 or 16 dB, respectively [32]. The maximum symbol rate for our frequency comb with a spacing of 12.5 GHz is 12.5 GBd at Nyquist channel spacing [8]. For this symbol rate, the SNR is approximately equal to the OCNR. Thus, our frequency comb provides a carrier quality that is sufficient for an SNR larger than 25.8 dB for all carriers.

6. Conclusion

We present a scheme for the generation of broad frequency combs via self-phase modulation. Differently broadened spectra are sliced and combined to a compound spectrum. Unstable, low-power spectral portions with a low CNR are removed and replaced with stable parts of the differently broadened spectra. A mode locked laser with a mode-linewidth of approximately 1 kHz serves as a seed spectrum. The generated frequency comb has 325 optical carriers and covers a bandwidth larger than 4 THz. We measured carrier-power to noise-power-density ratios (CNR) between 118.6 dBHz and 104.6 dBHz with 1 Hz reference bandwidth (39.6 dB(0.1nm) and 25.9 dB(0.1nm) with 0.1 nm reference bandwidth) for the regions of interest. The carrier quality suffices for transmission of multiple terabit/s using 16QAM [8], [16] with aggregate data rates of up to 32.5 Tbit/s [8].

Acknowledgment

We thank Dr. Marc Eichhorn of the French-German Research Institute of Saint-Louis for fruitful discussions on the measurement of laser linewidth and self-phase modulation, and for his support in the interpretation of the results. Special thanks go to Dr. Erel Granot of the Ariel University Center of Samaria in Israel for his support in the evaluation of the linewidth measurements.

References

[1] J. L. Hall, "Optical frequency measurement: 40 years of technology revolutions," *IEEE J. Sel. Topics Quantum Electron.*, vol. 6, no. 6, pp. 1136–1144, Nov./Dec. 2000.
[2] T. Udem, R. Holzwarth, and T. W. Hansch, "Optical frequency metrology," *Nature*, vol. 416, no. 6877, pp. 233–237, Mar. 2002.
[3] S. T. Cundiff and A. M. Weiner, "Optical arbitrary waveform generation," *Nat. Photon.*, vol. 4, no. 11, pp. 760–766, Nov. 2010.
[4] T. M. Fortier, M. S. Kirchner, F. Quinlan, J. Taylor, J. C. Bergquist, T. Rosenband, N. Lemke, A. Ludlow, Y. Jiang, C. W. Oates, and S. A. Diddams, "Generation of ultrastable microwaves via optical frequency division," *Nat. Photon.*, vol. 5, no. 7, pp. 425–429, Jul. 2011.
[5] P. J. Delfyett, S. Gee, M.-T. Choi, H. Izadpanah, W. Lee, S. Ozharar, F. Quinlan, and T. Yilmaz, "Optical frequency combs from semiconductor lasers and applications in ultrawideband signal processing and communications," *J. Lightwave Technol.*, vol. 24, no. 7, pp. 2701–2719, Jul. 2006.
[6] N. K. Fontaine, G. Raybon, B. Guan, A. L. Adamiecki, P. Winzer, R. Ryf, A. Konczykowska, F. Jorge, J.-Y. Dupuy, L. L. Buhl, S. Chandrasekhar, R. Delbue, P. Pupalaikis, and A. Sureka, "228-GHz coherent receiver using digital optical bandwidth interleaving and reception of 214-GBd (856-Gb/s) PDM-QPSK," presented at the European Conference Optical Communication, Amsterdam, The Netherlands, 2012, Paper Th.3.A.1.
[7] T. Kawanishi, S. Oikawa, K. Higuma, and M. Izutsu, "Electrically tunable delay line using an optical single-side-band modulator," *IEEE Photon. Technol. Lett.*, vol. 14, no. 10, pp. 1454–1456, Oct. 2002.
[8] D. Hillerkuss, R. Schmogrow, M. Meyer, S. Wolf, M. Jordan, P. Kleinow, N. Lindenmann, P. C. Schindler, A. Melikyan, X. Yang, S. Ben-Ezra, B. Nebendahl, M. Dreschmann, J. Meyer, F. Parmigiani, P. Petropoulos, B. Resan, A. Oehler, K. Weingarten, L. Altenhain, T. Ellermeyer, M. Moeller, M. Huebner, J. Becker, C. Koos, W. Freude, and J. Leuthold, "Single-laser 32.5 Tbit/s Nyquist WDM transmission," *J. Opt. Commun. Netw.*, vol. 4, no. 10, pp. 715–723, Oct. 2012.
[9] A. D. Ellis and F. C. G. Gunning, "Spectral density enhancement using coherent WDM," *IEEE Photon. Technol. Lett.*, vol. 17, no. 2, pp. 504–506, Feb. 2005.
[10] T. Sakamoto, T. Kawanishi, and M. Izutsu, "Widely wavelength-tunable ultra-flat frequency comb generation using conventional dual-drive Mach–Zehnder modulator," *Electron. Lett.*, vol. 43, no. 19, pp. 1039–1040, Sep. 2007.
[11] Y. Ma, Q. Yang, Y. Tang, S. Chen, and W. Shieh, "1-Tb/s single-channel coherent optical OFDM transmission over 600-km SSMF fiber with subwavelength bandwidth access," *Opt. Exp.*, vol. 17, no. 11, pp. 9421–9427, May 2009.
[12] S. Chandrasekhar, L. Xiang, B. Zhu, and D. W. Peckham, "Transmission of a 1.2-Tb/s 24-carrier no-guard-interval coherent OFDM superchannel over 7200-km of ultra-large-area fiber," presented at the European Conference Optical Communication, Vienna, Austria, 2009, Paper PD2.6.
[13] D. Hillerkuss, T. Schellinger, R. Schmogrow, M. Winter, T. Vallaitis, R. Bonk, A. Marculescu, J. Li, M. Dreschmann, J. Meyer, S. Ben Ezra, N. Narkiss, B. Nebendahl, F. Parmigiani, P. Petropoulos, B. Resan, K. Weingarten, T. Ellermeyer, J. Lutz, M. Möller, M. Hübner, J. Becker, C. Koos, W. Freude, and J. Leuthold, "Single source optical OFDM transmitter and optical FFT receiver demonstrated at line rates of 5.4 and 10.8 Tbit/s," presented at the Optical Fiber Communication Conference, San Diego, CA, USA, 2010, Paper PDPC1.
[14] X. Yang, D. Richardson, and P. Petropoulos, "Nonlinear generation of ultra-flat broadened spectrum based on adaptive pulse shaping," presented at the European Conference Optical Communication, Geneva, Switzerland, 2011, Paper We.7.A.2.
[15] J. Pfeifle, C. Weimann, F. Bach, J. Riemensberger, K. Hartinger, D. Hillerkuss, M. Jordan, R. Holtzwarth, T. J. Kippenberg, J. Leuthold, W. Freude, and C. Koos, "Microresonator-based optical frequency combs for high-bitrate WDM data transmission," presented at the Optical Fiber Communication Conference, Los Angeles, CA, USA, 2012, Paper OW1C.4.

[16] D. Hillerkuss, R. Schmogrow, T. Schellinger, M. Jordan, M. Winter, G. Huber, T. Vallaitis, R. Bonk, P. Kleinow, F. Frey, M. Roeger, S. Koenig, A. Ludwig, A. Marculescu, J. Li, M. Hoh, M. Dreschmann, J. Meyer, S. Ben Ezra, N. Narkiss, B. Nebendahl, F. Parmigiani, P. Petropoulos, B. Resan, A. Oehler, K. Weingarten, T. Ellermeyer, J. Lutz, M. Moeller, M. Huebner, J. Becker, C. Koos, W. Freude, and J. Leuthold, "26 Tbits^{-1} line-rate super-channel transmission utilizing all-optical fast Fourier transform processing," *Nat. Photon.*, vol. 5, no. 6, pp. 364–371, Jun. 2011.
[17] L. Boivin, M. C. Nuss, W. H. Knox, and J. B. Stark, "206-channel chirped-pulse wavelength-division multiplexed transmitter," *Electron. Lett.*, vol. 33, no. 10, pp. 827–829, May 1997.
[18] S. Kray, F. Spöler, T. Hellerer, and H. Kurz, "Electronically controlled coherent linear optical sampling for optical coherence tomography," *Opt. Exp.*, vol. 18, no. 10, pp. 9976–9990, May 2010.
[19] I. Coddington, W. C. Swann, L. Nenadovic, and N. R. Newbury, "Rapid and precise absolute distance measurements at long range," *Nat. Photon.*, vol. 3, no. 6, pp. 351–356, Jun. 2009.
[20] L. Xiang, S. Chandrasekhar, Z. Benyuan, and D. W. Peckham, "Efficient digital coherent detection of a 1.2-Tb/s 24-carrier no-guard-interval CO-OFDM signal by simultaneously detecting multiple carriers per sampling," presented at the Optical Fiber Communication Conference, San Diego, CA, USA, 2010, Paper OWO2.
[21] G. Bosco, A. Carena, V. Curri, P. Poggiolini, and F. Forghieri, "Performance limits of Nyquist-WDM and CO-OFDM in high-speed PM-QPSK systems," *IEEE Photon. Technol. Lett.*, vol. 22, no. 15, pp. 1129–1131, Aug. 2010.
[22] R. Schmogrow, M. Winter, M. Meyer, D. Hillerkuss, S. Wolf, B. Baeuerle, A. Ludwig, B. Nebendahl, S. Ben-Ezra, J. Meyer, M. Dreschmann, M. Huebner, J. Becker, C. Koos, W. Freude, and J. Leuthold, "Real-time Nyquist pulse generation beyond 100 Gbit/s and its relation to OFDM," *Opt. Exp.*, vol. 20, no. 1, pp. 317–337, Jan. 2012.
[23] R. Schmogrow, M. Meyer, S. Wolf, B. Nebendahl, D. Hillerkuss, B. Baeuerle, M. Dreschmann, J. Meyer, M. Huebner, J. Becker, C. Koos, W. Freude, and J. Leuthold, "150 Gbit/s real-time Nyquist pulse transmission over 150 km SSMF enhanced by DSP with dynamic precision," presented at the Optical Fiber Communication Conference, Los Angeles, CA, USA, 2012, Paper OM2A.6.
[24] A. Mishra, R. Schmogrow, I. Tomkos, D. Hillerkuss, C. Koos, W. Freude, and J. Leuthold, "Flexible RF-based comb generator," *IEEE Photon. Technol. Lett.*, vol. 25, no. 7, pp. 701–704, Apr. 2013.
[25] P. Del'Haye, T. Herr, E. Gavartin, M. L. Gorodetsky, R. Holzwarth, and T. J. Kippenberg, "Octave spanning tunable frequency comb from a microresonator," *Phys. Rev. Lett.*, vol. 107, no. 6, pp. 063901-1–063901-4, Aug. 2011.
[26] M. A. Foster, J. S. Levy, O. Kuzucu, K. Saha, M. Lipson, and A. L. Gaeta, "Silicon-based monolithic optical frequency comb source," *Opt. Exp.*, vol. 19, no. 15, pp. 14 233–14 239, Jul. 2011.
[27] R. H. Stolen and C. Lin, "Self-phase-modulation in silica optical fibers," *Phys. Rev. A, At. Mol. Opt. Phys.*, vol. 17, no. 4, pp. 1448–1453, Apr. 1978.
[28] G. Agrawal, *Nonlinear Fiber Optics*. Amsterdam, The Netherlands: Elsevier, 2001.
[29] E. L. Goldstein, L. Eskildsen, and A. F. Elrefaie, "Performance implications of component crosstalk in transparent lightwave networks," *IEEE Photon. Technol. Lett.*, vol. 6, no. 5, pp. 657–660, May 1994.
[30] L. Richter, H. Mandelberg, M. Kruger, and P. McGrath, "Linewidth determination from self-heterodyne measurements with subcoherence delay times," *IEEE J. Quantum Electron.*, vol. QE-22, no. 11, pp. 2070–2074, Nov. 1986.
[31] D. Derickson and C. Hentschel, *Fiber Optic Test and Measurement*. Englewood Cliffs, NJ, USA: Prentice-Hall, 1998.
[32] R. J. Essiambre, G. Kramer, P. J. Winzer, G. J. Foschini, and B. Goebel, "Capacity limits of optical fiber networks," *J. Lightwave Technol.*, vol. 28, no. 4, pp. 662–701, Feb. 2010.